Materials Chemistry and Physics 174 (2016) 41–53

Contents lists available at ScienceDirect

Materials Chemistry and Physics

journal homepage: www.elsevier.com/locate/matchemphys

Effects of intrinsic defects on effective work function for Ni/HfO_2 interfaces

Kehua Zhong [a, c, **], Guigui Xu [a, b], Jian-Min Zhang [a, c], Renyuan Liao [a, c], Zhigao Huang [a, c, *]

[a] Fujian Provincial Key Laboratory of Quantum Manipulation and New Energy Materials, College of Physics and Energy, Fujian Normal University, Fuzhou 350117, China
[b] Concord University College, Fujian Normal University, Fuzhou 350117, China
[c] Fujian Provincial Collaborative Innovation Center for Optoelectronic Semiconductors and Efficient Devices, Xiamen 361005, China

HIGHLIGHTS

- The interfaces with O–Ni combining bonds are more energetically favorable.
- The change of EWF is 1.8 eV for Hf terminated interfaces with Ni substitution for Hf.
- The change of EWF is 3.2 eV for Hf terminated interfaces with Hf vacancy.
- The change of EWF is 2.0 eV for O terminated interfaces with O vacancy.
- Results are explained by interface dipole density, ionic valence and occupied states.

ARTICLE INFO

Article history:
Received 12 January 2015
Received in revised form
15 February 2016
Accepted 16 February 2016
Available online 28 February 2016

Keywords:
Ni/HfO_2 interface
First-principles
Effective work function
Intrinsic defect

ABSTRACT

The effective work functions and formation energies for Ni/HfO_2 interfaces with and without defects, including interfacial intrinsic atom substitution and atom vacancy in interfacial layer were studied by first-principles methods based on density functional theory (DFT). The calculated results of the formation energies indicate that the interfaces with O–Ni combining bonds in the interfacial region are more energetically favorable and a small amount O vacancy is comparatively easy to form in O–Ni interface, especially under O-rich situation. Moreover, the results of our calculations also reveal that, (1) the effective work functions strongly depend on the type of interface, interface roughness and atom substitution content in the interface region; (2) for Hf–Ni interfaces, two calculated effective work functions without and with Ni substitutions in whole interfacial Hf layer are good for *n*MOS and *p*MOS effective work function (EWF) engineering, respectively; (3) the EWFs are sensitive to Hf vacancy rather than Ni vacancy in interfacial layer for Hf–Ni interfaces; (4) oxygen vacancies can result in a decrease of effective work function for O–Ni interfaces. Additionally, we establish an expected theoretical relationship that variations of the EWFs are in proportion to that of interface dipole density. Finally, ionic valence state and occupied state are used to qualitatively analyze and explain the effects of interfacial defects on the EWF in metal-oxide interfaces. Our work suggests that controlling interfacial intrinsic atom substitution and interface roughness are attractive and promising ways for modulating the effective work function of Ni/HfO_2 interfaces.

1. Introduction

To solve the problems arising from the aggressive size downscaling of metal-oxide-semiconductor field-effect transistor (MOSFET), both high dielectric constant "high-*k*" gate dielectric and metal gate electrode are required to replace the traditional SiO_2 gate dielectric and polycrystalline Si, respectively [1,2]. Because of its high dielectric constant, excellent thermal stability and

* Corresponding author. Fujian Provincial Key Laboratory of Quantum Manipulation and New Energy Materials, College of Physics and Energy, Fujian Normal University, Fuzhou 350117, China.
** Corresponding author. Fujian Provincial Key Laboratory of Quantum Manipulation and New Energy Materials, College of Physics and Energy, Fujian Normal University, Fuzhou 350117, China.
E-mail addresses: khzhong@fjnu.edu.cn (K. Zhong), zghuang@fjnu.edu.cn (Z. Huang).

http://dx.doi.org/10.1016/j.matchemphys.2016.02.049
0254-0584/

compatibility with various technical requirements, Hafnium oxide (HfO_2) has emerged as one of the most preferred gate oxides in high-*k* metal gate technology [2–4]. While for desirable metal gate, an appropriate effective work function needs to satisfy the requirement that it lies near the valence and conduction band edges of Si substrate (about 4.1 eV and 5.2 eV for negative MOS [*n*MOS] and positive MOS [*p*MOS], respectively) [5]. There have been many studies [6–16] on tuning the effective work function (EWF) of metal-high-*k* gate stacks and several accompanying possible modulation methods for the EWF, such as binary alloys [6], bilayer metal gate technology [7], and atomic dopant [8–15]. However, even so, the EWF is difficult to control, especially for *p*MOS, due to its extreme sensitivity to a number of factors that can alter metal-oxide interfacial electronic properties. Typically, during the actual sample deposition and integration procedures, interfacial effects, such as lattice mismatch, interface reconstruction, defect accumulation, interfacial bond formation and dipoles formation, make achieving a suitable metal gate a challenge [3,17,18], because the EWF of the metal gate could differ from its vacuum work function [19–21].

It has been reported that the EWF may strongly depend on the processing conditions that the device is subjected to [22–26]. For instance, oxygen-rich or oxygen-deficient conditions can result in different interfaces [27]. Moreover, in the actual experimental deposition process, defects will inevitably exist in the interface of metal-oxide. For example, although the defect formation energies is relatively high, oxygen vacancies in HfO_2 can be easily generated in actual devices with the help of the oxidation of underlying silicon [28,29]. The so-called extended Frenkel pair defect is found to be quite unfavorable for some metals like TiN [30] and Pt [31], it has been found to be energetically favorable for several other metals such as molybdenum [32], rhodium and nickle [33], and hafnium metal [34]. The defects such as oxygen vacancy and interstitial atoms segregating near metal-HfO_2 interfaces, cause variation of interface EWF via changing the interface dipole strength [22,35–37]. Furthermore, the EWF of *p*MOS gate is sensitive to oxygen vacancy inside the metal/high-*k* interface [19,22]. As noted above, it is well known that defects in the interface strongly influence the electronic properties of metal-oxide interface. They can act as *n*- or *p*-type dopants that reduce or raise the EWF of interface, respectively. Therefore, an in-depth understanding of the physical origin for the effects of defects on the EWF is of great importance for the present and future MOSFET technology. Recently, the metal-HfO_2 interfaces with oxygen vacancy have been investigated using first-principles calculations [18,31,32,36,37]. Cho et al. have found that oxygen vacancies are strongly attracted to the interface, in particular for the metal with high EWF, and the interfacial segregation of vacancies significantly affects the EWF of metals [31,36]. Vacuum work function of metal surface can be modulated by surface dipole layer [38–40], similarly, the EWF of metal-oxide interfaces can be tuned by interface dipole layer. Very recently, the interface dipole formed in metal-oxide interface was reported to strongly affect the EWF of the system [41–43]. Tse et al. found that a barrier height being about 0.9 eV lower than those of nonpolar interfaces was produced by a large interface dipole for O-rich metal-HfO_2 interfaces [41]. Bokdam et al. investigated the EWF in TiN/HfO_2 interface consisting of either Ti–O or N–Hf interface bonds. They found that the replacement of O-rich bonds for N-rich interface bonds caused a decline of the EWF by up to 0.36 eV, which is attributed to the formation of opposing interface dipoles [43].

In fact, experimentally, the interfacial intrinsic atom substitution and interface roughness caused by the interfacial atom vacancy can be easily formed in the interfacial layer of metal-HfO_2 interface. These defects should greatly change the EWF. Controlling interface roughness can thus be a good way to tune the EWF. Unfortunately, mechanism how intrinsic defects affect the EWF of metal-HfO_2 is still unclear. This motivates us to investigate the impacts of the mixture of metal atoms from each side and interface roughness in metal-HfO_2 interface. Furthermore, Ni is a typical gate metal material due to its high work function, thermal stability and good compatibility with high dielectric constant medium material.

In this paper, we systematically investigate the impacts of intrinsic defects on the EWF of the typical fcc-Ni(001)/c-HfO_2(001) interfaces using first-principles calculations. Defects including mixture of Ni and Hf atoms, oxygen vacancy, Ni or Hf vacancy at interface region are considered. Two types of Ni(001)/HfO_2(001) interface were considered: the HfO_2 terminated with Hf atom layer (Hf–Ni interface) and the HfO_2 terminated with O atom layer (O–Ni interface). The defective interfaces include Hf–Ni interface with Ni atoms substituting for the interfacial Hf atoms (referred as S_{Ni} interface), Hf–Ni interface with Ni vacancy in interfacial Ni layer (referred as V_{Ni} interface), Hf–Ni interface with Hf vacancy in interfacial Hf layer (referred as V_{Hf} interface), and O–Ni interface with O vacancy in interfacial O layer (referred as V_O interface). We assess the stabilities of pure interfaces, S_{Ni}, V_{Ni}, V_{Hf}, and V_O interfaces with various substitution or vacancy content under different growth environments according to formation energy of interfaces. We also find out the relationship between EWF and interface dipole. The calculated results indicate that the interfaces with O–Ni combining bonds in the interfacial region are energetically favored and a small amount O vacancy is comparatively easy to form in O–Ni interface, especially under O-rich situation. Furthermore, it is found that the mixture of Ni and Hf atoms, Hf vacancy and oxygen vacancy in the interfacial layer all play significant roles in the EWF. Finally, the expected theoretical relationship that the variations of EWFs are in proportion to that of interface dipole density is established. The EWFs' shifts caused by the interfacial defects are qualitatively explained in term of ionic valence state and occupied state.

This paper is organized as follows. In Section 2, we describe the details of the method for all calculations. In Section 3, we firstly calculate the formation energies for Hf–Ni and O–Ni interfaces with and without defects include interfacial atom substitution and atom vacancy and discuss the stability of those interfaces. Then we calculate the EWF and interface dipole for Hf–Ni and O–Ni interfaces with various defects. Additionally, we qualitatively analyze and explain the effects of interfacial defects on the EWF using ionic valence state and occupied state. Finally, we conclude our paper with a summary of what we found.

2. Method

All the calculations were performed using Vienna *ab initio* simulation package (VASP) with projector augmented wave approach [44–50]. The exchange correlation energy was calculated using PW91 generalized gradient approximation (GGA) [45]. With these pseudopotentials, the valence configuration was $6s^2 5d^2$ for Hf atoms, the valence configuration was $4s^2 3d^8$ for Ni atoms and $2s^2 2p^4$ for oxygen atoms. Spin polarization was included, and the plane-wave basis cutoff was set at 400 eV. Our calculated lattice constant for bulk cubic-HfO_2 is $a_{HfO_2} = 5.025$Å, which is slightly lower than the experimental value of 5.08 Å [51]. Fcc-Ni(001) has very good lattice match to cubic-HfO_2(001) after relative 45 ° rotations. For Hf–Ni (O–Ni) interfaces, we employ the 2×2 interface supercells with 9 layers of Ni atoms, 7 layers of Hf atoms, and 6 (or 8) layers of O atoms and no vacuum [48]. The half supercells of these two types of interfaces without defects were shown in Fig. 1(a), (b), respectively. A $4 \times 4 \times 1$ Monkhorst-Pack *k*-mesh was adopted for the calculations. To find the equilibrium structure of interfaces, the lateral lattice parameters were set to be the value of

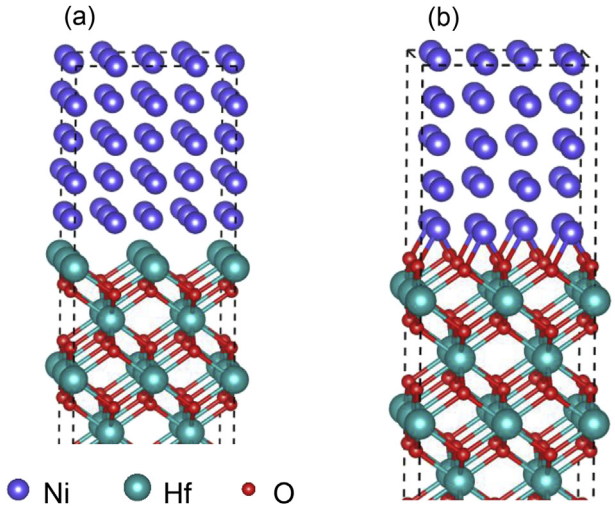

Fig. 1. Crystal structure illustrations for half of a 2 × 2 supercell of Hf–Ni (a), and O–Ni (b) interfaces without defects.

bulk ($a_{HfO_2}/\sqrt{2} = 3.553$Å) during the relaxation. Moreover, the Ni atoms, the top four (five) atomic layers of the HfO_2 surface for Hf–Ni (O–Ni) interfaces, and the vertical lattice vector were allowed to relax to minimize the DFT total energy. The atoms were fully relaxed through the conjugate-gradient algorithm until the residual force on each atom is less than 0.02 eV/Å.

3. Results and discussion

3.1. Formation energy of interfaces with defects

The relative stability of an actual interface with or without defects is generally given by the interface formation energy E_{form}, which is defined as [52].

$$E_{form} = \frac{E_{Ni/HfO_2} - \left(nE_{Ni} + mE_{HfO_2} \pm l\mu_O\right)}{2A}, \quad (1)$$

where E_{Ni/HfO_2} is the total energy of the interface supercell with or without defects, E_{Ni} and E_{HfO_2} is the total energies per Ni and HfO_2 bulk unit respectively, n and m denotes the numbers of Ni atoms and HfO_2 bulk units in the supercell respectively, and l indicates the corresponding number of oxygen atoms that has been added to (+) or removed (−) from the supercell. A is the area of the interface supercell. μ_O denotes the chemical potential of oxygen, and is determined as follows

$$\frac{1}{2}\left(E_{O_2} + H_f\right) \le \mu_O \le \frac{1}{2}E_{O_2}, \quad (2)$$

where H_f=−10.83 eV denotes the formation enthalpy (by convention is negative) per formula unit for c-HfO_2, defined as

$$H_f = E_{HfO_2} - \left(E_{Hf} + E_{O_2}\right), \quad (3)$$

E_{O_2} and E_{Hf} are the DFT total energies per oxygen molecule and Hf atom in *hcp*-Hf bulk, respectively.

Fig. 2 shows the formation energies versus chemical potential of oxygen for Hf–Ni and O–Ni interfaces without or with defects. From Fig. 2 (a), it is found that S_{Ni} interface with θ = 1.00 ML (the whole interfacial Hf layer is substituted by Ni atoms) has the lowest formation energy in all the μ_O ranges. It is noted that the formation

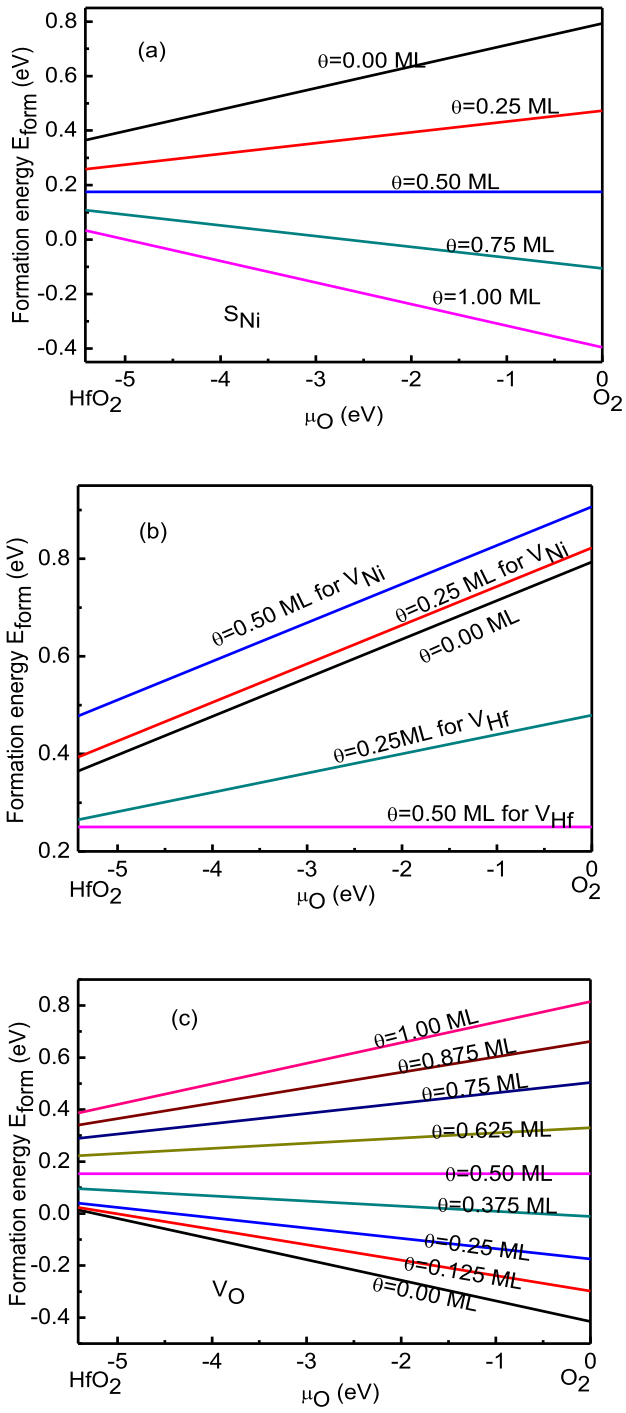

Fig. 2. The formation energy E_{form} as a function of oxygen chemical potential μ_O for various defects in (a) Hf–Ni interface with Ni substitute for Hf atoms (S_{Ni}), (b) Hf–Ni interface with Ni or Hf vacancy (V_{Ni} or V_{Hf}), and (c) O–Ni interface with O vacancy (V_O). θ denotes substitution or vacancy content. θ = 0.00 ML represents interfaces without defects.

energy decreases with the increase of θ under the same growth condition, especially in the O-rich conditions. Obviously, this indicates that Ni–O bond is more energetically favorable than Hf–O bond, and Ni prefers to substitute for Hf. Further, substituting Hf with Ni becomes more easily when the growth atmosphere evolves to be extremely O rich. This can be explained qualitatively by the

much larger electronegativity of Ni than that of Hf. Additionally, we can also see clearly from Fig. 2(a) that, the energy of S_{Ni} for $\theta < 0.50$ ML increases monotonically with μ_O, on the contrary, it decreases with increasing μ_O for $\theta > 0.50$ ML. In particular, the energy of S_{Ni} with $\theta = 1.00$ ML is nearly close to that of O–Ni interface without O vacancy given as the case of $\theta = 0.00$ ML in Fig. 2(c). This may be due to the dominant role of different interfacial metal atoms. When $\theta < 0.50$ ML, Hf has a larger proportion than Ni and contributes more to interface structure. However, as $\theta > 0.50$ ML, the contribution of Ni to interface structure becomes more. Ultimately, a maximal substitution of Hf by Ni ($\theta = 1.00$ ML) turns the original Hf–Ni interface into similar O–Ni interface. Therefore, from another perspective, it is suggested that O–Ni interface may be superior to Hf–Ni interface during Ni/HfO_2 interface preparation.

From Fig. 2(b), it can be seen that, for all V_{Ni} and V_{Hf} interfaces except V_{Hf} with $\theta = 0.50$ ML, the formation energy increases as μ_O increases. Moreover, compared to the interface without defect, Ni vacancy existing in interfacial Ni layer for Hf–Ni interface causes energetically unstable, and the more Ni vacancy the higher the formation energy. However, Hf vacancy in Hf interfacial layer decreases the formation energy. Contrary to the case for Ni vacancy, the more Hf vacancy causes a lower formation energy. As shown in Fig. 2(b), for the V_{Hf} interface with $\theta = 0.50$ ML, Hf vacancy has the lowest formation energy for all the μ_O ranges. This implies that Hf vacancy is prone to exist in Hf–Ni interface, but Ni vacancy is hard to form in Ni interfacial region. It may be thought of as a result of different nearest neighbor number of metallic and ionic bonds for Ni and Hf atoms. The nearest neighbor atoms of Ni atoms have 10 metallic bonds. But, the nearest neighbor atoms of Hf atoms have 4 metallic and 4 ionic bonds.

For V_O interfaces, as can be seen clearly from Fig. 2(c), the formation of O vacancy defect would only become energetically unfavorable under the same growth condition, which is similar to previous research of O vacancy in HfO_2 [53]. Moreover, the formation energy increases as vacancy content θ increases, and the changing amplitude also increases gradually as μ_O increases. This can be considered that there are plenty of oxygen atoms in the O-rich region, so that oxygen atom will prefer to fill interfacial vacancy due to oxygen's leaving if an interfacial O vacancy occurs. Therefore, E_{form} increases more quickly as μ_O increases. In addition, similar to the case for S_{Ni} interface in Fig. 2(a), the changing trend of E_{form} versus μ_O in V_O interface for $\theta < 0.50$ ML is opposite to that for $\theta > 0.50$ ML. For V_O in O–Ni interface for $\theta < 0.50$ ML, O vacancy becomes more likely to occur under O-rich situation than under O-deficient situation. In this case, if there exists oxygen vacancy in interface region, the number of Ni–O bonds will decrease, and Hf–Ni interaction may appear. But, for smaller amount of O vacancy, Ni–O bonds may make a predominant contribution to interface structure. So the relationship between E_{form} and μ_O for interfaces with low O vacancy is similar to that for O–Ni interface without defects. On the other hand, for those V_O interfaces with θ being in the range of $\theta > 0.50$ ML, it is less likely that O vacancy in the interfacial region will be formed under O-rich situation than under O-deficient situation. As shown in Fig. 2(c), the formation energy increases much quickly with increasing value of μ_O. Additionally, it is noted that the change tendency of E_{form} with increasing value of μ_O for $\theta = 1.00$ ML is nearly close to that for Hf–Ni interface without any defects given as the case of $\theta = 0.00$ ML in Fig. 2(a). It can be explained as follows: with the increase of O vacancy in range of $\theta > 0.50$ ML, Ni–Hf interaction enhances generally, finally it leads to form Ni–Hf bond. Moreover, as O vacancy content further increases, Ni–Hf bonds increase but Ni–O bonds decrease. When $\theta = 1.00$ ML, the ionic bonding in O–Ni interface goes over into the metallic bonding, which is similar to Hf–Ni interface shown in Fig. 2 (a). These results show that a small amount O vacancy in the interface region is comparatively easy to form in O–Ni interface, especially under O-rich situation.

The relative stability of an interface is given by its interfacial formation energy. The smaller the interfacial formation energy, the more stable the interface structure. On the contrary, the too high formation energy would prevent two materials to form interface. As shown in Fig. 2(a) and (b), for Hf–Ni interface without defects and all V_{Ni} interfaces, the formation energy increases as μ_O increases. Furthermore, the more Ni vacancy the higher the formation energy. When the interfacial formation energy is too high under the O-rich growth condition, Ni would no longer be expected to wet the surface of HfO_2.

3.2. Effective work function of interfaces with defects

Fig. 3 shows a schematic of a typical band lineup for a metal-oxide interface. The interface EWF ϕ_{eff} is generally estimated as [15,27,48,52].

$$\phi_{eff} = \chi_{HfO_2} + E_g^{HfO_2} - \varphi_p, \tag{4}$$

where χ_{HfO_2} and $E_g^{HfO_2}$ is the electron affinity and band gap of HfO_2, respectively. The p-type Schottky-barrier height (SBH) φ_P is the difference between Ni Fermi energy and the oxide valence band maximum. The φ_P for interface can be obtained by using the standard "bulk-plus-lineup" [54,55] procedure, which is usually split into two terms:

$$\varphi_p = \left(E_F^{Ni} - E_{VBM}^{HfO_2}\right) + \Delta V, \tag{5}$$

where the first term is the energy difference between the metal Fermi energy and the oxide valence band maximum which are measured relative to the respective average of electrostatic potential, as obtained from two independent bulk calculations. The second term ΔV is the difference between the double macroscopic average of the electrostatic potential residing in Ni and HfO_2 bulk-like-regions respectively, which can be obtained using the double macroscopic average technique [56]. Combined Eq. (5) with Eq. (4), the EWF can be evaluated through the equation

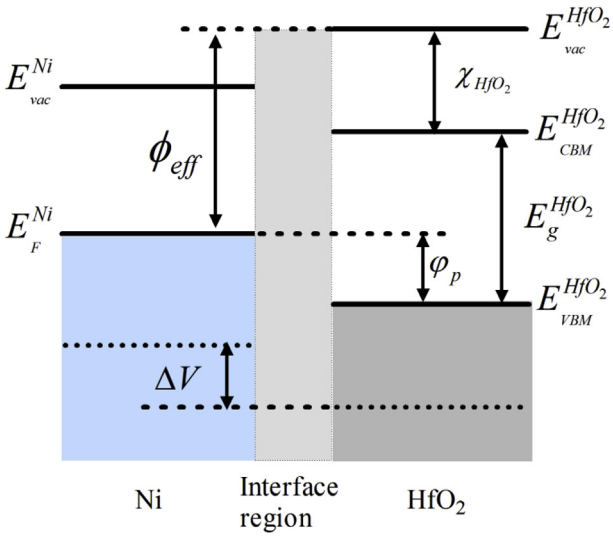

Fig. 3. The schematic view of band alignment at Ni/HfO_2 interface.

$$\phi_{eff} = \left(\chi_{HfO_2} + E_g^{HfO_2} + E_{VBM}^{HfO_2} - E_F^{Ni}\right) - \Delta V = \Delta E_{bulk} + D. \quad (6)$$

In Eq. (6), the first term ΔE_{bulk} represents intrinsic bulk electronic structure of the two bulk components. It is not related to the interface structure. While, the second term D summarizes the effect of the dipole barrier in the interface which is affected by all the interface effects, including chemical composition, defects in interface region and so on. In the calculation, the experimental values with $\chi_{HfO_2} = 2.5$ and $E_g^{HfO_2} = 5.7$ eV were used [21]. As DFT underestimates the oxide gap, a GW correction of 1.23 eV for HfO_2 valence band maximum has been considered [15,21]. And for Ni, 0.29 eV correction was added by comparing our DFT calculation value (4.93 eV) and the experimental value (5.22 eV) for the effective work function of Ni(001) surface. The overall corrections, −0.94 eV, are used in the following EWF calculation. Here, the negative sign means the corrections will decrease the EWF. Our calculations of *p*-type SBH for Hf–Ni and O–Ni interfaces of Ni(001)/HfO_2(001) are 4.00 and 2.06 eV respectively, which are close to the results of Ni(001)/ZrO_2(001) (3.80 and 2.13 eV) [27], indicating that our calculations are reliable for the EWF of interfaces.

Fig. 4(a) shows the EWF (ϕ_{eff}) as a function of Ni substitution content θ for Hf–Ni interfaces. Fig. 4(b) shows the EWF (ϕ_{eff}) as a function of Ni or Hf vacancy content θ for Hf–Ni interfaces. Fig. 4(c) shows the EWF (ϕ_{eff}) as a function of O vacancy content θ for O–Ni interfaces. From Fig. 4(a) and (c), the marked difference (about 2 eV) between the two effective work functions of Hf–Ni and O–Ni interfaces without defects can be observed clearly. This is due to their different types of chemical bond in interface region, more details can be found in Section 3.3. For S_{Ni} interfaces, it is found clearly from Fig. 4 (a) that the interfacial intrinsic atom substitution plays a significant role in determining the effective work function of the whole metal-oxide interface. For $\theta < 0.50$ ML, ϕ_{eff} increases with the increase of substitution content θ, and the maximal changed value of effective work function reaches about 1.8 eV being from 4.15 eV to 5.96 eV. Although there is a relatively slow decline with increasing θ for $\theta > 0.50$ ML, the value of ϕ_{eff} decreases from 5.96 eV ($\theta = 1.00$ ML) to 5.33 eV ($\theta = 0.50$ ML). However, substituting Hf with Ni for Hf–Ni interfaces with θ=0.00 ML ($\phi_{eff} = 4.15$ eV) and $\theta = 1.00$ ML ($\phi_{eff} = 5.33$ eV) may be good for *n*MOS and *p*MOS EWF engineering, respectively. Furthermore, substituting Hf with Ni for Hf–Ni interface becomes much easier to occur in O rich condition for θ>0.50 ML, as shown in Fig. 2 (a). This implies that alloying in interfacial metal layer is a simple practical way of modulating the ϕ_{eff} for Hf–Ni interface to satisfy the engineering requirement for metal gate technology. The difference between two changing trends of ϕ_{eff} in ranges of θ<0.50 ML and θ>0.50 ML may be a result of comprehensive effect of two parts of interface dipole, one is from the ionic Hf–O (Ni–O) bonds in interfacial metal layer, and the other is from the positively charged interfacial metal layer and its image charge in Ni side. And we will discuss the effects of the two parts of interface dipole in more detail in subsequent Section 3.3.

From Fig. 4(b), we can see evidently that ϕ_{eff} is not sensitive to Ni vacancy in interfacial Ni layer for Hf–Ni interface. Conversely, it strongly depends on Hf vacancy in interfacial Hf layer. It almost increases linearly with the increase of Hf vacancy content θ, and a considerably big increment of 3.2 eV corresponds to the vacancy content of θ=0.50*ML*. Moreover, relative to the interface without defect, V_{Hf} interfaces are more energetically stable, and the more Hf vacancy content the more stable interface, shown in Fig. 2 (b). The calculated results indicate that the effects of different metal atom vacancy in interfacial layer on the EWF differ widely, which implies that controlling the vacancy content of suitable interfacial metal atom vacancy is also a possible way of tuning the EWF of metal-oxide interface. In other words, the interface roughness in the region of interface is quite important and should be taken with great concern in the EWF engineering in metal/high-*k* gate stack.

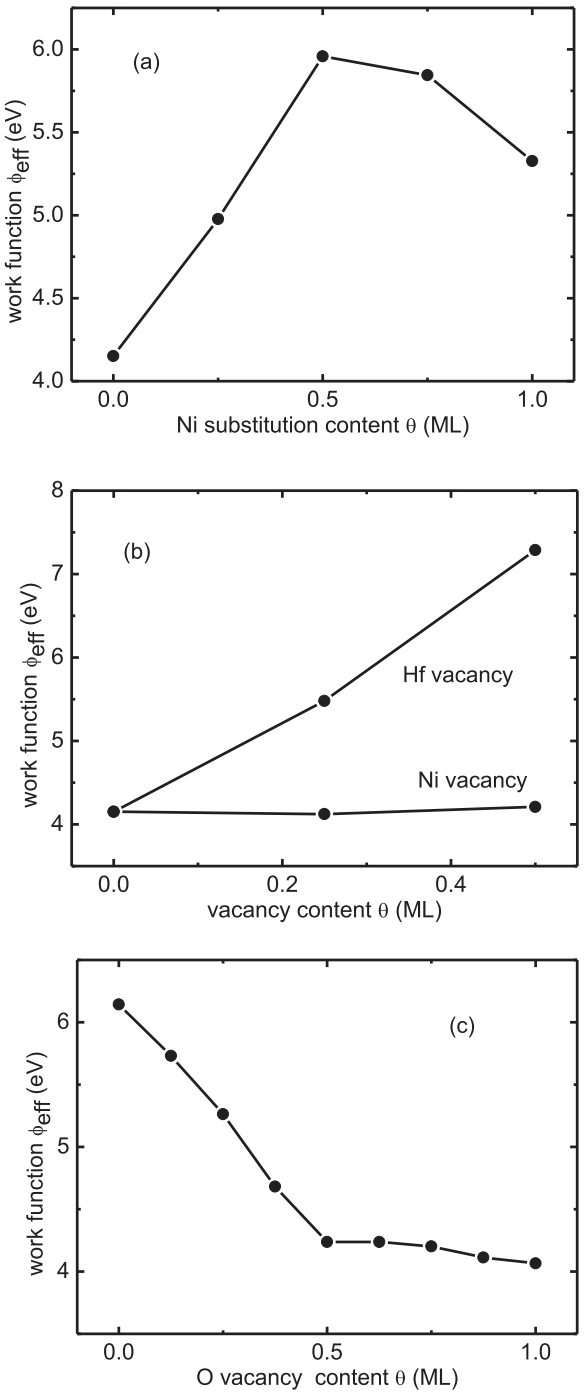

Fig. 4. Effective work function ϕ_{eff} for (a) S_{Ni} of Hf–Ni interface, (b) V_{Ni} and V_{Hf} of Hf–Ni interfaces, and (c) V_O of O–Ni interface with various substitution or vacancy content θ.

From Fig. 4(c), we can clearly find that the removal of oxygen results in the decrease of EWF for V_O of O–Ni interface as a whole. Moreover, the changing trend shows an initial linear rapid decrease for θ<0.50 ML, a more gradual and also almost linear decrease for θ>0.50 ML. This behavior is associated to the corresponding change trend for interface dipole which is related to electron transfer and

interfacial oxygen-metal chemical bonds, as discussed in Section 3.3. The value of ϕ_{eff} as a function of O vacancy content θ indicates that impact of O vacancy on the EWF mainly lies in low O vacancy content range of θ<0.50 ML, where the value of φ_{eff} changes from 6.1 eV ($\theta = 0.00$ ML) to 4.2 eV ($\theta = 0.50$ ML). Meanwhile, it can be also found from Fig. 2(c) that V_O interfaces with low O vacancy content are energetically favorable. This suggests that controlling O vacancy content is also a possible solution to modulate the EWF of O–Ni interface.

3.3. Interface dipole of interface

According to Eq. (6), the change of effective work function $\Delta\phi_{eff}$ stems from the changes of two bulk electronic structures and interface structure. If the change of the interfacial structure do not affect the two bulk components, $\Delta\phi_{eff}$ will be determined by the change of interface dipole barrier ΔD. Moreover, the change of interface dipole barrier ΔD is proportional to interface dipole density change ΔP that is similar to the behavior of surface dipole density [40], that is, $\Delta\phi_{eff}$ satisfies the relation of $\Delta\phi_{eff} \propto -\Delta P$. The electronic displacement and dipole formation in the interface can be observed by looking at the electron density of the entire interface minus the electron densities of the two separate constituent materials. The electron displacement in the formation of interface is defined as

$$\Delta n_{inter}(x,y,z) = n_{inter}(x,y,z) - n_{Ni}(x,y,z) - n_{HfO_2}(x,y,z). \quad (7)$$

Here, $n_{inter}(x,y,z)$, $n_{Ni}(x,y,z)$ and $n_{HfO_2}(x,y,z)$ are the electron density distributions of the interface, the clean metal and oxide layer, respectively.

Since only the component perpendicular to the interface is relevant, it is convenient to work with plane averaged charge density difference of the valence electron $\Delta\lambda(z) = \frac{1}{A}\int \Delta n_{inter}(x,y,z)\ dx\ dy$. Z denotes the direction which is parallel to interface normal. The interface dipole density P can be given as [43,57].

$$P = -\int_{z_0}^{c/2} \Delta\lambda(z)\cdot z\cdot dz. \quad (8)$$

The center of metal Ni is chosen to be at z_0, and c/2 corresponds to the center of HfO_2. The negative sign is introduced because positive regions of $\Delta\lambda(z)$ are actually negatively charged.

The defects inside the interface may give different results in charge transfer and dipole density. The change of charge transfer due to defect in the interface is represented by the electron redistribution. And the redistribution is most straightforwardly described through the electron density difference. Fig. 5 shows the plane averaged charge density difference of valence electron $\Delta\lambda(z)$ for S_{Ni} of Hf–Ni interface. The variation of interface dipole density derived from Eq. (8) could be applied to explain the change of EWF. The variation of the interface dipole density and the EWF as a function of defect content θ are simultaneously presented in Fig. 6. The theoretical prediction of $\Delta\phi_{eff} \propto -\Delta P$ can be seen in the figure.

For S_{Ni} of Hf–Ni interface, several features from Fig. 5 can be identified as follows: (1) metallic bonding between Hf and Ni atoms exists in the interface region for Hf–Ni interface without defect, namely, S_{Ni} with $\theta = 0.00$ ML. A well screening role coming from interfacial Hf atom layer permits the charge transfer only to take place in the zone between interfacial Hf and Ni atoms layers, as shown in Fig. 5. Ni and Hf atoms in the interface lose electrons, and the lost electrons are aggregated in the intermediate bonding zone between Ni and Hf atoms in the interface. However, when Ni

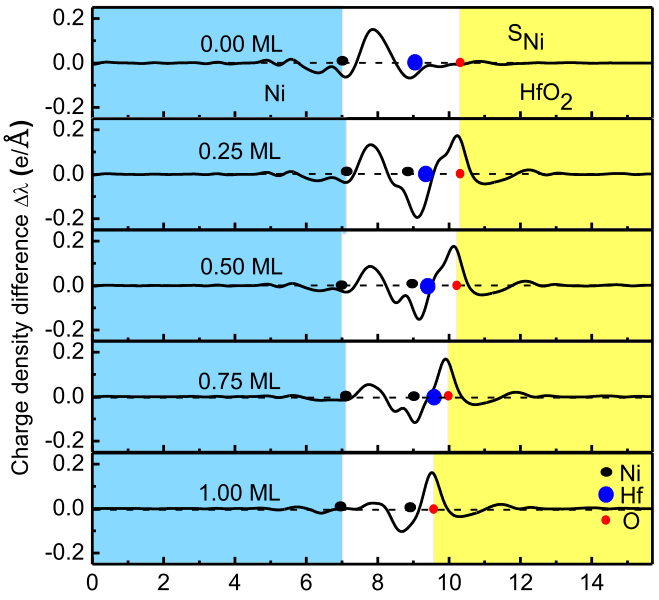

Fig. 5. Plane averaged charge density difference of valence electron $\Delta\lambda(z)$ for S_{Ni} of Hf–Ni interface.

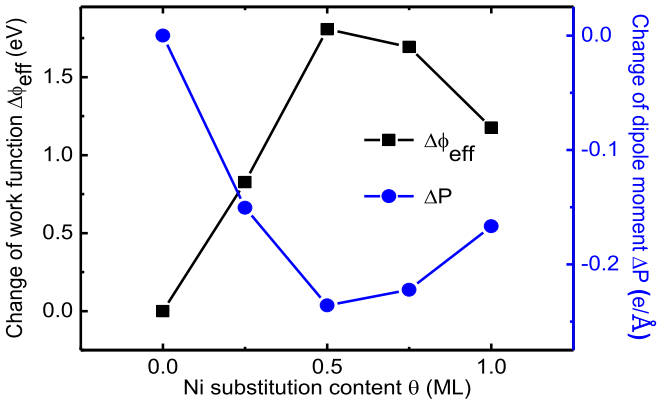

Fig. 6. Variations of interface dipole density and effective work function as a function of substitution content θ for S_{Ni} of Hf–Ni interface.

substitutes for Hf in interface region, due to Ni's stronger electronegativity and different oxidation state, it can actually destroy the screening of interfacial Hf atom layer for the charge transfer from interfacial zone to interior of HfO_2, so electronic rearrangement is visible for $\theta = 0.25$ ML. And there is a considerable electron accumulation near interfacial O atom layer, thus the ionic bonding between O and Ni in interface layer appears. Consequently, there are two types of chemical bond coexisting in interface region. One is ionic Hf–O (Ni–O) bond, the other is metallic bonding between Hf and Ni atom. Accordingly, the total interface dipole comprises two parts: the first one, which is from the ionic Hf–O (Ni–O) bonds in interfacial metal layer, is pointing from Ni to HfO_2 and makes the EWF increase; the second one, which is from the positively charged interfacial Ni and Hf atoms mixing layer and its image charge in Ni side, is pointing from HfO_2 to Ni and makes the EWF decrease. So for θ<0.50 ML, both factors act cooperatively to increase the EWF, as shown in Fig. 6. (2) However, in high Ni substitution range of θ>0.50 ML, the EWF decreases conversely. Its opposite change trend as substitution content θ can also be understood as follows: on the one hand, with a continual increase of Ni substitution, the electronegativity of metal mixing layer would continue to enhance.

Thus the part of dipole from metallic bonds continues to decrease accordingly. On the other hand, the interface zone between interfacial Ni and O layers becomes narrower with the increase of Ni substitution for θ>0.50 ML, as shown in Fig. 5. The distance of the z axis between interfacial metal atoms mixing layer and O layer becomes smaller as θ increases. Moreover, the amount of charge transfer also has a small decrease. Therefore, both effects above make a great drop in the part of dipole from Hf–O (Ni–O) ionic bond, which makes the EWF decrease. Eventually, the drop in part of dipole from ionic bonds surpasses the continual decrease of the part of dipole from metallic bonds. Consequently, the change of total dipole causes a decline of the EWF relative to that for $\theta = 0.50$ ML, but the EWF has still a rise relative to that for Hf–Ni interface without Ni substitution ($\theta = 0.00$ ML). The change of total dipole as a function of all substitution content θ is presented in Fig. 6. It can well explain the difference between two changing trends of ϕ_{eff} for θ<0.50 ML and θ>0.50 ML (3) Additionally, with the increase of θ, the electron accumulation has gradually moved from the original region (between Ni and Hf layers in the interface) into the area near O layer. In turn, now the losing and gaining of electrons mainly come from the mixing metal layer and interfacial O layer, respectively. Accordingly, the chemical bonds in the interface change from metallic bonds to ionic bonds, as seen in Fig. 5. Moreover, it can be seen from Fig. 5, for all S_{Ni} interfaces, dipoles are primarily due to the contributions of the interface layer Ni, Hf and O atoms, while the contributions of the layer which is most close to the interface are rather small, and that of the farther layers are negligible.

Fig. 7(a) and (b) show the plane averaged charge density differences $\Delta\lambda(z)$ for V_{Hf} and V_{Ni} interfaces, respectively. One can easily notice that: (1) for V_{Hf} interface, $\Delta\lambda(z)$ changes rapidly. Hf vacancy in interface leads to a smaller screening role of interfacial Hf layer on the electron in intermediate zone. In addition, O atoms which are near to Hf vacancy have a strong electronegativity. As a result, the electron accumulation moves from intermediate zone between interfacial Ni and Hf atoms layers to that area near interfacial O layer. Furthermore, the dipole layer moves to HfO_2 side, as shown in Fig. 7(a). Then, being similar to the case of S_{Ni}, there exist two kinds of chemical bonds that ionic bond and metallic bond between Hf and Ni atom. As Hf vacancy content increases, Hf atoms in defect layer move away from Ni atoms to O atoms, and the electron transfer between interfacial Ni and Hf layers reduces rapidly, while the electron accumulation moves to the region near O atom layer. For example, for $\theta = 0.50$ ML, there is hardly any electron accumulation but only electron depletion in region between interfacial Ni and Hf, and the dipole is mainly from ionic bond. The large variation of the EWF caused by variation of total dipole is clearly seen in Fig. 8. (2) While for V_{Ni} interfaces, $\Delta\lambda(z)$ only has small change. Moreover, despite the increase of Ni vacancy, the chemical bond in interface region remains metallic bond between Hf and Ni atom, which can be seen clearly from the charge density differences $\Delta\lambda(z)$ in Fig. 7(b). This may be due to the almost constant electronegativity in Ni side. Even if Ni atoms are removed, the electronegativity of Ni side is almost not changed because of Ni's delocalized electrons. And Ni's removal affects the electron distribution in intermediate zone very weakly. As a result, the total dipole changes hardly as a whole, so the EWF does hardly too, as shown in Fig. 8.

The plane averaged charge density differences $\Delta\lambda(z)$ for V_O interfaces are shown in Fig. 9. From the figure, it is found that ionic bonding between O and Ni atoms exists in interface region for O–Ni interface without O vacancy ($\theta = 0.00$ ML). The interface dipoles are formed due to the electron accumulation near O layer and the electron depletion near Ni layer. As can be seen from the figure, unlike V_{Hf}, for all interfaces, the dipole layer does not move to HfO_2 side because of a very good screening role coming from interfacial Hf layer, which hinders the electron in intermediate zone to penetrate into HfO_2 side. From the figure, we can also find that intermediate zone becomes narrower with increasing θ. Moreover, the curves of $\Delta\lambda$ on the distance from Ni bulk z mainly represent the characteristic of ionic bond for all interfaces with θ<0.50 ML. While for interfaces with θ>0.50 ML, it represents the characteristic of metallic bond. For the interfaces with θ<0.50 ML, the gradually decreasing electronegativity of interfacial metal atoms due to O vacancies gives rise to a decline of dipole from ionic bond as θ increasing. It corresponds to the gradual reduction of amount of the

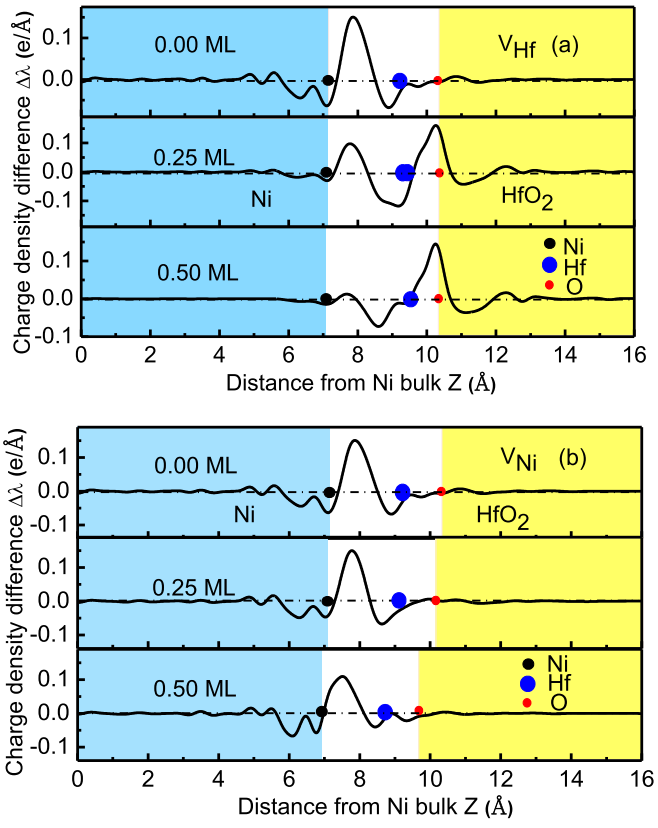

Fig. 7. Plane averaged charge density difference of valence electron $\Delta\lambda(z)$ for (a) V_{Ni} and (b) V_{Hf} of Hf–Ni interfaces.

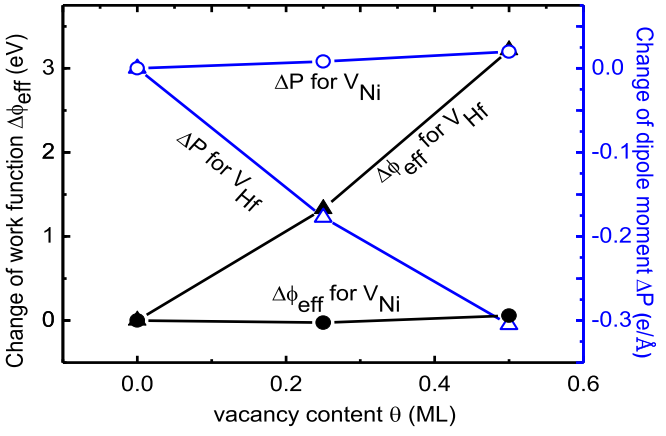

Fig. 8. Variations of interface dipole density and effective work function as a function of vacancy content θ for V_{Ni} and V_{Hf} of Hf–Ni interfaces.

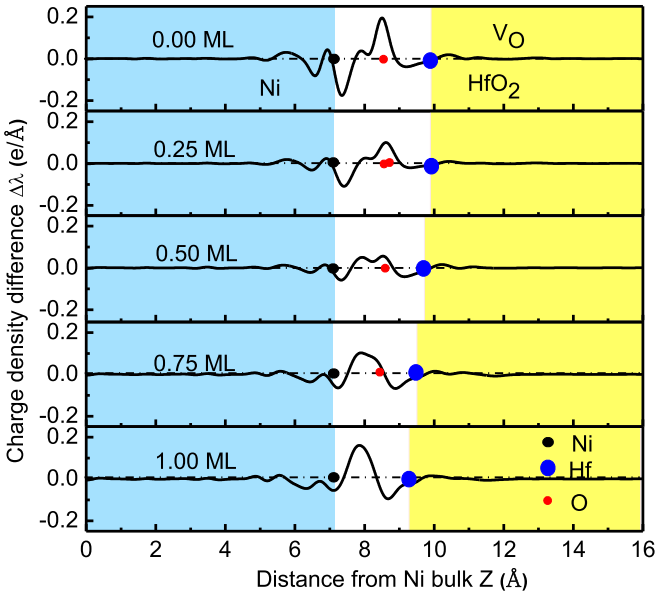

Fig. 9. Plane averaged charge density difference of valence electron $\Delta\lambda(z)$ for V_O of O–Ni interface.

electron accumulation or depletion, as shown in Fig. 9. When the increment of the oxygen vacancies reaches a critical value, the metallic bond appears. As a result, there exist two types of dipole which are from ionic bond and metallic bond respectively. But, it is noteworthy that even the decline of the part of dipole from ionic bond, it still plays a dominant role in the whole dipole for θ<0.50 ML. So it is can be seen from Fig. 9 that the curves of $\Delta\lambda(z)$ mainly represent the characteristic of ionic bond. Consequently, the amount of the whole dipole decreases with increasing θ, accordingly, the EWF decreases, as shown in Fig. 10. However, for interfaces with θ>0.50 ML, with further increase of O vacancies the supportive role of O atoms for forming O–Ni interface decreases. As a result, the distance between interfacial Ni layer and Hf layer becomes much closer, and their metallic interaction strengthens. On the other hand, further increase of O vacancies weakens ionic interaction between metal atoms and oxygen atoms. So the part of dipole from ionic bond becomes smaller and smaller and finally vanishes for θ = 1.00 ML. Contrary to the case for θ<0.50 ML, the part of dipole from metallic bond plays a dominant role in the whole dipole. This corresponds to the phenomenon that the curves

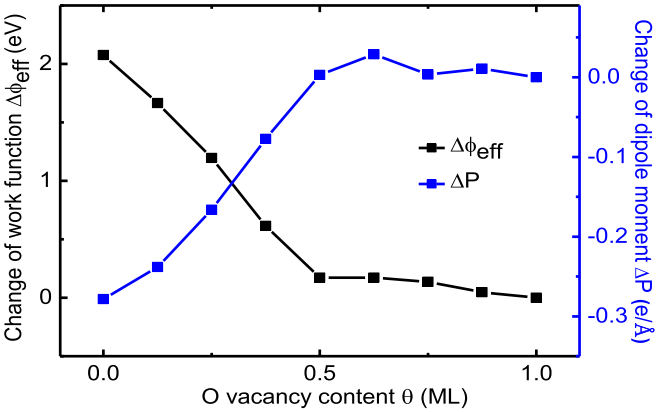

Fig. 10. Variations of interface dipole density and effective work function as a function of vacancy content θ for V_O of O–Ni interface.

of $\Delta\lambda(z)$ mainly represent the characteristic of metallic bond for θ>0.50 ML. Moreover, despite there is some increased amount of charge transfer, the distance between interfacial Ni layer and Hf layer becomes much closer. As a result, the total interface dipole and the EWF change slightly, as shown in Fig. 10.

3.4. Effective work function, ionic valence state and occupied state

In a metal-oxide interface, controlling the EWF of metal is actually to manipulate the relative position of Fermi level (E_F), and the EWF is associated with the atomic site-projected density of states (PDOS). We now try to explain qualitatively the mechanism of the above EWF's shifts in terms of local bonding and changes of interfacial ionic valence state due to atom vacancy or substitution defects. Fig. 11(a)-(f) show the total density of states (TDOS) and the PDOS of different atoms residing in different layers for S_{Ni} interfaces with θ from 0.00 ML to 1.00 ML, respectively. Fig. 12(a)-(d), Fig. 13(a)-(d) and Fig. 14(a)-(h) are those for V_{Hf},V_{Ni} and V_O interfaces, respectively. In Figs. 11(a), 12(a), 13(a) and 14(a), the energies of all interfaces align at the deep energy level of bulk oxide. As shown in Fig. 11(a), it can be seen clearly that the position of E_F in the band gap of bulk oxide is strongly dependent on mixing ratios of interfacial metal mixing layer. From Fig. 11 (b)-(f), as a whole, substitution of Ni for Hf in interfacial layer shifts the Fermi level towards valence-band maximum (VBM) of HfO_2, resulting in substitution of Ni for Hf acting as an acceptor dopant (*p*-type doping). The changing trend of the Fermi level for different Ni substitution contents gives a qualitative account of the EWF behavior. We can also find that interface effects are restricted to the atomic planes in contact for all interfaces, which corresponds to the case of plane averaged charge density difference shown in Fig. 5. The PDOSs for interfacial Ni, Hf, O and substituted Ni atoms are perturbed by the formation of interface and alloying in interfacial metal layer. In energy range between E_F and VBM of HfO_2, it can be found that some occupied states are formed in substituted Ni, interface Hf and O layers. Furthermore, for θ<0.50 ML, the PDOSs indicate that the interactions between interfacial atoms are mainly limited to substituted Ni, interfacial Ni and Hf atoms. There exist evident occupied states in the interfacial Hf atoms, which suggests that strong metallic bonding appears between the interfacial Ni and Hf atoms. Moreover, there is no sign of bonding between substituted Ni atoms and interfacial O atoms. In contrast, for $\theta\geq$0.50 ML, the bonding between interfacial O and substituted Ni atoms in interface layer arises, and enhances with increasing θ, which indicates that ionic bonding exists between the interfacial Ni and O atoms.

Substitution of Ni for Hf in interface would cause interfacial charge redistributions and the change of oxygen-metal chemical bonds. The change of charge distributions will be directly reflected in the change of ionic valence state. To examine the change of ionic valence state due to the electron transfer at the interface, we calculate the number of electrons around the interfacial Hf, O and substituted Ni atoms using the Bader charge analysis, and compare the results with those for the inner atoms. For θ = 0.00 ML, we find that interfacial Hf is positively charged, $Hf^{+3.42}$ for θ = 0.00 ML, then its oxidation state slightly reduces to $Hf^{+3.30}$ and $Hf^{+3.27}$ for θ = 0.25 ML and 0.50 ML, respectively, but remains unchanged for θ>0.50 ML. This corresponds to the PDOS for interfacial Hf atoms in Fig. 11. Differently, substituted Ni is slightly positively charged, $Ni^{+0.41}$ when θ = 0.25 ML, then its charge increase to $Ni^{+0.67}$ for θ = 0.50 ML, and there appears a new higher oxidation state $Ni^{+0.98}$ forθ>0.50 ML. To adjust the lower oxidation states of substituted Ni relative to the case for θ = 0.00 ML than Hf's, interfacial O atoms near substituted Ni atoms lose about 0.2 electrons for $\theta\leq$0.50 ML, but a half of interfacial O atoms lose about 0.52 electrons for θ = 0.75 ML, and then all interfacial O atoms lose about 0.52

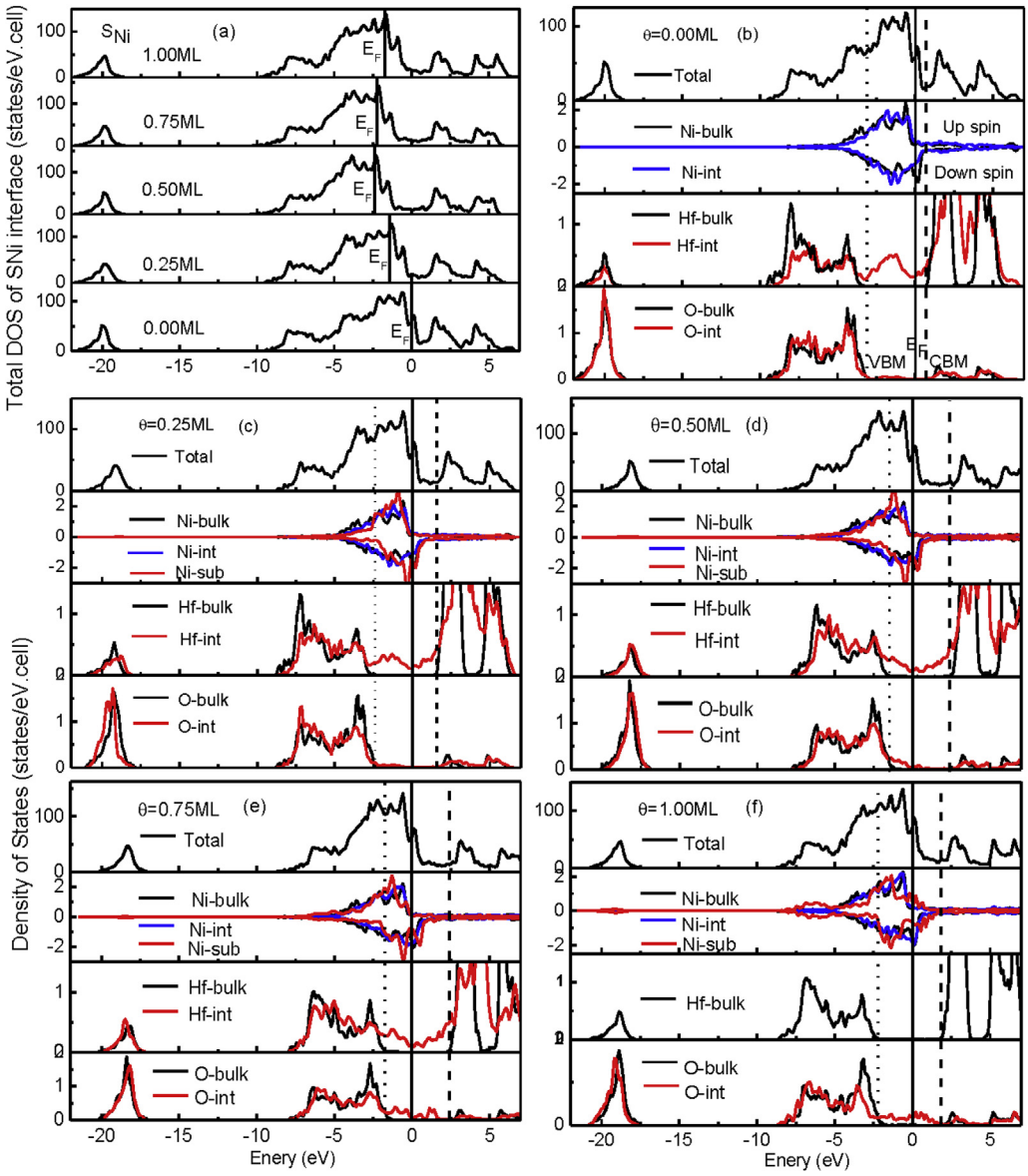

Fig. 11. Total density of states (TDOS) (a) and atomic site-projected density of states (PDOS) for S_{Ni} interfaces with (b) substitution content $\theta = 0.00$ ML, (c) 0.25 ML, (d) 0.50 ML, (e) 0.75 ML, (f) 1.00 ML. In the PDOS, the symbols are defined as follows: for Ni and Hf in bulk region (Ni-bulk, Hf-bulk), interface metal Hf, Ni and O (Hf-int, Ni-int and O-int), substituted Ni (Ni-sub), oxygen in bulk region (O-bulk). The solid, dot and dash lines denote Fermi energy of interface, VBM and CBM of HfO_2, respectively. The energies of all interfaces in (a) align at the deep energy level of bulk oxide.

electrons when$\theta = 1.00$ ML. This indicates that a new lower anion valence state appears for θ>0.50 ML. This new lower valence state corresponds to the interfacial O's DOS in Fig. 11(e) and (f), which indicates further that there exists a strong ionic bonding between the interfacial Ni and O atoms for θ>0.50 ML.

In S_{Ni} interfaces, these changes of interfacial ionic valence state would eventually affect the change of total interface dipole, which has been discussed in Section 3.3. The interface dipole will generate a corresponding electric field, which is equivalent to adding an extra bias voltage to the original one. As a result, it will give an additional potential energy. Moreover, substitution of Ni generates lower cation oxidation state. As a result, the interface acquire more holes to realize the transition from *n*-type to *p*-type for Ni/HfO_2 interface, which leads to more stable *p*-type occupied states near VBM. Therefore, the interface dipole and the occupied states in the interfacial Hf and O atoms result in a shifting of Ni's DOS relative to the band structures of HfO_2, as shown in Fig. 11(b)-(f). In other words, they alter the position of interface Fermi level (E_F) in the oxide band gap, and hence shift the EWF.

For V_{Hf} interfaces, as shown in Fig. 12(a), the Fermi level in the band gap of bulk oxide depends critically on Hf vacancy content θ. Similar for the case of S_{Ni} interfaces, Hf vacancy in interfacial layer shifts the Fermi level to VBM of HfO_2, and acts as an acceptor dopant (*p*-type doping). From Fig. 12(b)-(d), we can also find that interface effects are restricted to the interfacial Ni, Hf and O atomic planes. The PDOSs for interfacial Ni, Hf and O atoms indicate that a small amount of Hf vacancy for$\theta = 0.25$ ML weakens the metallic bonds between interfacial Hf and Ni but enhances those ionic bonds between remaining interfacial Hf atoms and their neighboring O atoms. However, on the whole, it does not destroy the interfacial metallic bonding type. When Hf vacancy increases to $\theta = 0.50$ ML, the changes of interaction among interfacial Hf, Ni and O atoms continue to enhance and eventually lead to only ionic bonding in interface, as shown in Fig. 7 (a).

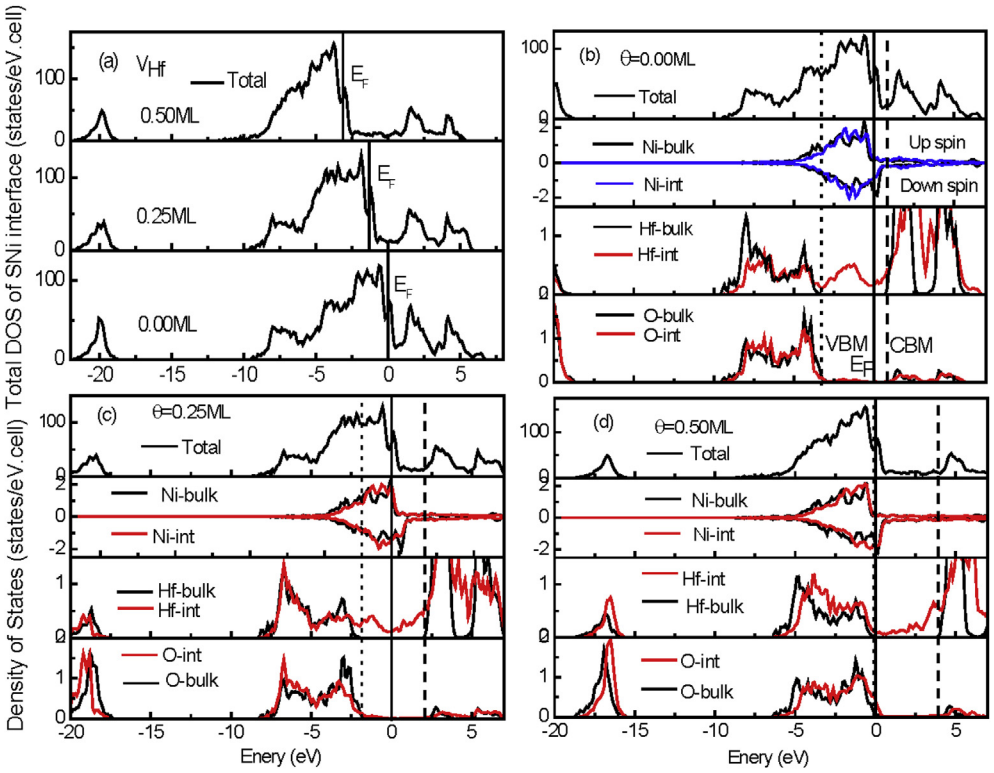

Fig. 12. Total density of states (TDOS) (a) and atomic site-projected density of states (PDOS) for V_{Hf} interfaces with (b) vacancy content $\theta = 0.00$ ML, (c) 0.25 ML, (d) 0.50 ML. In the PDOS, the symbols are defined as follows: for Ni and Hf in bulk region (Ni-bulk, Hf-bulk), interface metal Hf, Ni and O (Hf-int, Ni-int, O-int), oxygen in bulk region (O-bulk). The solid, dot and dash lines denote Fermi energy of interface, VBM and CBM of HfO_2, respectively. The energies of all interfaces in (a) align at the deep energy level of bulk oxide.

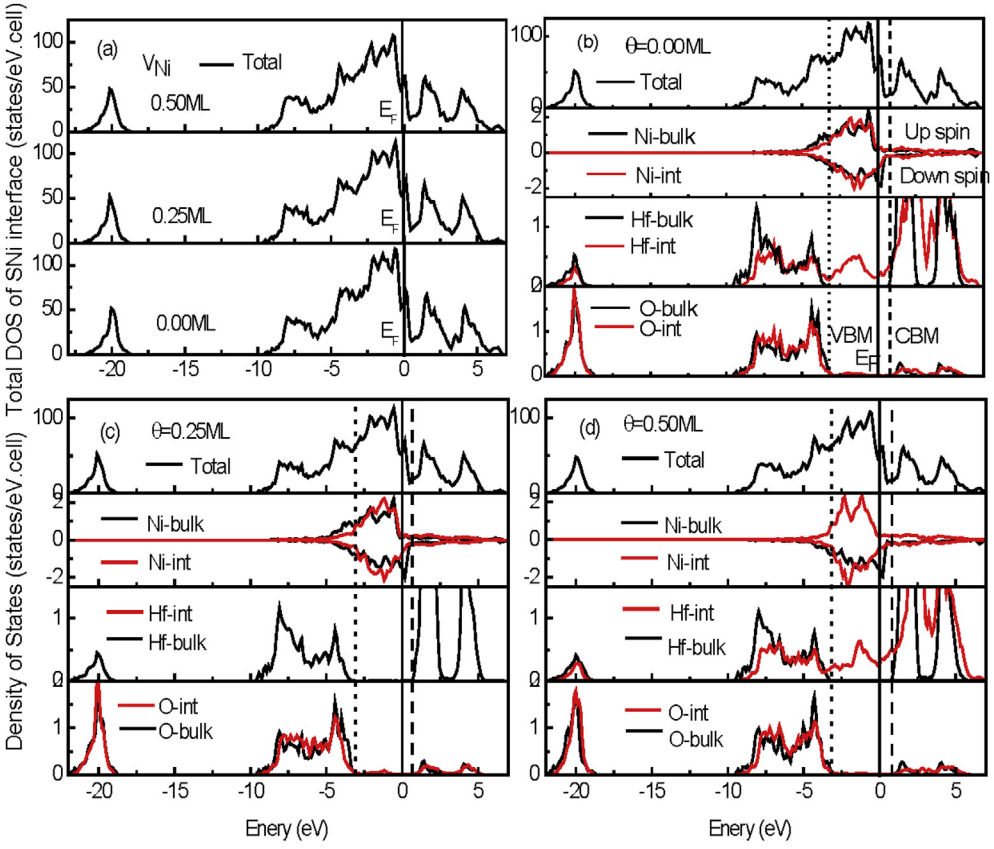

Fig. 13. Total density of states (TDOS) (a) and atomic site-projected density of states (PDOS) for V_{Ni} interfaces with (b) vacancy content $\theta = 0.00$ ML, (c) 0.25 ML, (d) 0.50 ML. In the PDOS, the symbols are defined as follows: for Ni and Hf in bulk region (Ni-bulk, Hf-bulk), interface metal Hf, Ni and O (Hf-int, Ni-int and O-int), and oxygen in bulk region (O-bulk). The solid, dot and dash lines denote Fermi energy of interface, VBM and CBM of HfO_2, respectively. The energies of all interfaces in (a) align at the deep energy level of bulk oxide.

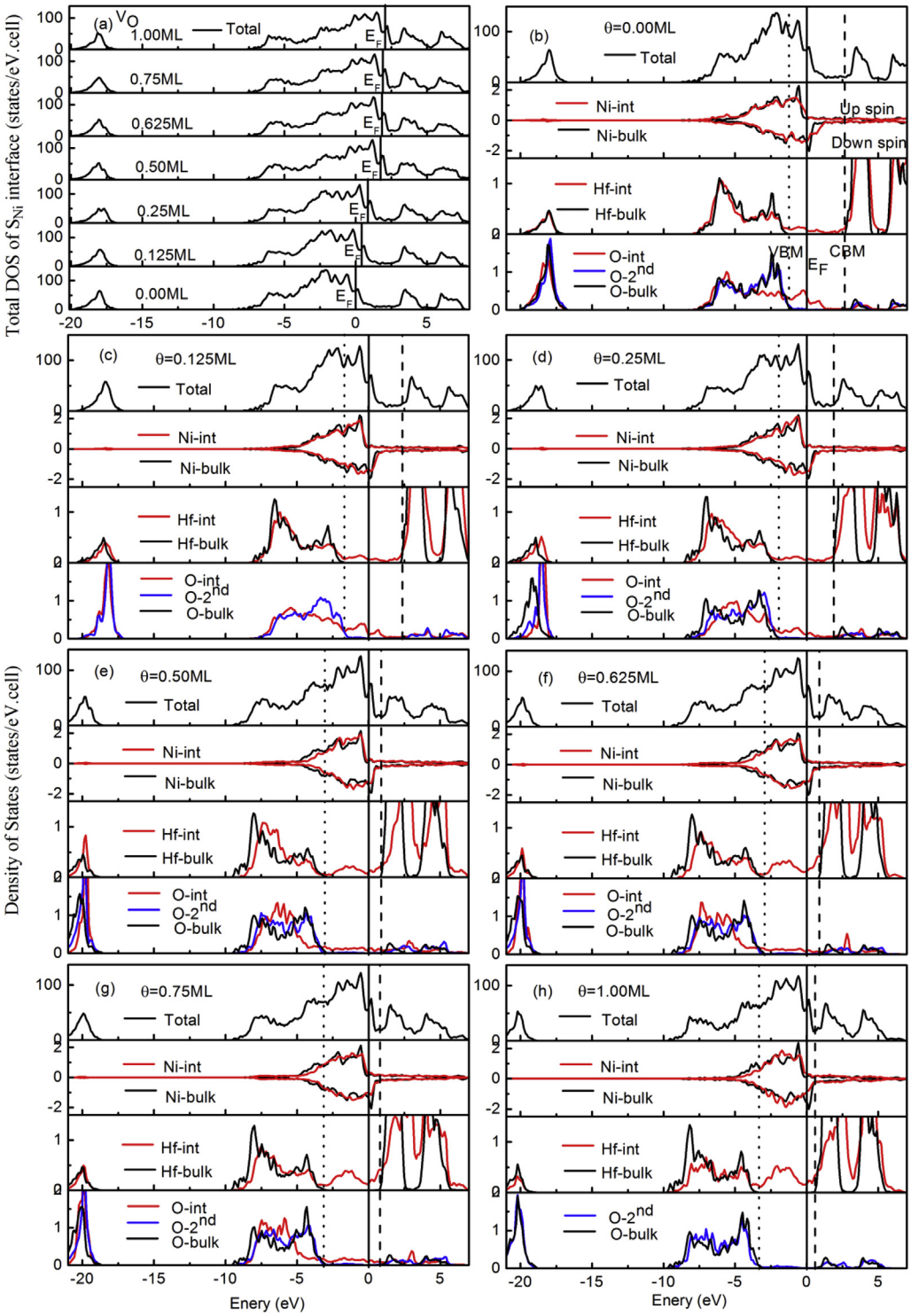

Fig. 14. Total density of states (TDOS) (a) and atomic site-projected density of states (PDOS) for V_O interfaces with (b) vacancy content $\theta = 0.00$ ML, (c) 0.125 ML, (d) 0.25 ML, (e) 0.50 ML, (f) 0.625 ML, (g) 0.75 ML, (h) 1.00 ML. In the PDOS, the symbols are defined as follows: for Ni and Hf in bulk region (Ni-bulk, Hf-bulk), interface metal Hf and Ni (Hf-int, Ni-int), sub-interface oxygen (O-2nd), oxygen in bulk region (O-bulk). The solid, dot and dash lines denote Fermi energy of interface, VBM and CBM of HfO_2, respectively. The energies of all interfaces in (a) align at the deep energy level of bulk oxide.

The ionic valence state might have changed because of the electron gain and loss. Interfacial Ni is originally negatively charged in forming Hf–Ni interface, due to its stronger electronegativity than Hf's. However, Hf vacancy reduces the chemical bonding number of interfacial Hf and Ni, hence weaken the interaction between them. As a result, Ni's originally negatively charged character weakens along with it. For instance, for $\theta = 0.50$ ML, interfacial Ni's charge is $Ni^{-0.15}$, and Ni loses about 0.5 electrons relative to that in interface without defect. Moreover, remaining interfacial Hf atoms for $\theta = 0.50$ ML gain about 0.2 electrons, and its

neighboring O atom loses about 0.3 electrons relative to that for $\theta = 0.00$ ML. Their charges are $Hf^{+3.22}$ and $O^{-1.70}$, respectively. Similar to the case for S_{Ni} interfaces discussed above, these changes of ionic valence state directly affect original total interface dipole and the occupied states, and ultimately make interface's Fermi level move very close to the VBM of HfO_2, as shown in Fig. 6, thus the EWF is enhanced.

For V_{Ni} interfaces, however, the Fermi level acts differently from that for above V_{Hf} interfaces, it does not depend on Ni vacancy content and is fixed, as shown in Fig. 13(a). Consequently, the EWF changes little accordingly. Fig. 13(b)-(d) show the PDOS for interfacial Ni, Hf and O atoms. From the figure, it is observed that they are nearly not affected by Ni vacancies in interfacial layer. That is, these Ni vacancies do not alter the metallic bonding between Hf and Ni atoms in interface, but only generate a little perturbation.

Fig. 14(a)-(h) show total density of states (TDOS) and atomic site-projected density of states (PDOS) for V_O interfaces with vacancy content $\theta = 0.00$ ML, 0.125 ML, 0.25 ML, 0.50 ML, 0.625 ML, 0.75 ML and 1.00 ML. In contrast to the cases for S_{Ni} and V_{Hf} interfaces, for V_O interfaces, oxygen vacancy acts as a donor dopant (n-type doping), as shown in Fig. 14(a). The Fermi level in the band gap of bulk oxide is strongly dependent on O vacancy content θ, especially for θ<0.50 ML. It shifts towards the conduction band minimum (CBM) of HfO_2. From Fig. 14(b)-(g), we can find that for a small amount of O vacancy (θ<0.50 ML), interfacial Ni atoms mainly bond to their neighboring O atoms and their bonds weaken with increasing θ. While for θ>0.50 ML, the interaction between Ni and O becomes very weak. Instead, with increasing O vacancies the bonds between the interfacial Ni atoms and their neighboring Hf atoms are enhanced and the occupied states near CBM are increased. The type of chemical bond is turned from ionic bonding to metallic bonding, which is consistent with the results shown in Fig. 9.

O vacancy is commonly formed in the metal oxide interface [31,36]. Thus, the emergence of O vacancy means there are additional Ni and Hf dangling bonds around vacancy site, and it is equivalent to releasing electrons. Consequently, it makes all its neighboring Ni, O and Hf atoms gain electrons. For example, the original interfacial Ni cations in interface with $\theta = 0.25$ ML gain about 0.3 electrons relative to that in interface without O vacancy, but remain their positively charged features. However, when θ>0.50 ML, they turn into being negatively charged features. Finally, it becomes $Ni^{-0.8}$ for $\theta = 1.00$ ML. But for Hf, it always has a positive charge. Moreover, for θ<0.50 ML, its positive nature weakens because of gaining electrons, such as $Hf^{+3.96}$ for $\theta = 0.00$ ML but $Hf^{+3.31}$ for $\theta = 0.50$ ML. However, it has a little enhancement for θ>0.50 ML, such as $Hf^{+3.51}$ for $\theta = 1.00$ ML. Remaining O in interfacial layer has an increasing negative charge only for θ<0.50 ML, $O^{-1.43}$ for $\theta = 0.00$ ML and $O^{-1.65}$ for $\theta = 0.50$ ML, but remains unchanged for θ>0.50 ML. It agrees with those localized PDOS of interfacial O in Fig. 14(e)-(h). These changes of ionic valence state caused by O vacancy also affect the interface dipole. Moreover, compared to the cases for S_{Ni} and V_{Hf} interfaces above, it has an opposite effect on interface dipole. That is, it pushes E_F to CBM of HfO_2 and then makes the EWF decrease. At the same time, the change trend of interfacial ionic valence state for θ<0.50 ML is different from that forθ>0.50 ML, as described above. And this is consistent with the phenomenon that interfacial chemical bonding is turned from ionic bonding to metallic bonding, shown in Fig. 9. To sum up, the interface dipole and the p-type occupied states near CBM of HfO_2 result in a shift of Ni's DOS relative to the band structures of HfO_2, which explains nicely the change of the EWF in Fig. 4(c).

4. Conclusions

In summary, we systematically studied the EWF and formation energies for Hf–Ni and O–Ni interfaces with and without defects including interfacial intrinsic atom substitution and atom vacancy in interfacial layer using first-principle calculation. The calculated formation energies indicate that O–Ni combining bonds may energetically be superior to Hf–Ni combining bonds during Ni/HfO_2 interface preparation, and a small amount of O vacancy is comparatively easy to form in O–Ni interface, especially under O-rich condition; Hf vacancy is prone to exist in Hf–Ni interface while Ni vacancy is hard to form in Ni interfacial region. Moreover, our results show that the EWF strongly depends on the type of interfaces, interface roughness and atom substitution content in interfaces, and the EWF of O–Ni interface without defects is as higher as 2.0 eV than that of Hf–Ni interface without defects. For Hf–Ni interfaces, it is found that two calculated effective work functions of interfaces without and with Ni substitution for whole interfacial Hf layer are good for nMOS and pMOS effective work function (EWF) engineering. Farther, one notices that Hf and O vacancies give rise to a considerably large EWF changes while Ni vacancy leads to an insensitive change of EWF. In addition, we obtain an expected theoretical relationship that variations of the EWFs are in proportion to that of interface dipole density. Ionic valence state and occupied state are used to qualitatively analyze and explain the effects of interfacial defects on the EWF. Our work suggests that controlling interfacial intrinsic atom substitution or interface roughness is a very attractive and promising way for modulating the EWF of Ni/HfO_2 interfaces, which is significant for the metal gate technology and application.

Acknowledgments

This work is supported by the National Science Foundation of China (61574037, 61404029, 11404058, 11274064), National Key Project for Basic Research of China under Grant No. 2011CBA00200, Educational Department of Fujian Province, China (JA14092).

References

[1] G.D. Wilk, R.M. Wallace, J.M. Anthony, High-κ gate dielectrics: current status and materials properties considerations, J. Appl. Phys. 89 (2001) 5243.
[2] E.P. Gusev, V. Narayanan, M.M. Frank, Advanced high-κ dielectric stacks with polySi and metal gates: recent progress and current challenges, IBM J. Res. Dev. 50 (2006) 387.
[3] J. Robertson, High dielectric constant gate oxides for metal oxide Si transistors, Rep. Prog. Phys. 69 (2006) 327.
[4] 2007 International Technology Roadmap for Semiconductors, Semiconductor Industry Association, San Jose, CA, 2007, p. 2.
[5] Y.J. Oh, A.T. Lee, H.-K. Nob, K.J. Chang, Hybrid functional versus quasiparticle calculations for the Schottky barrier and effective work function at TiN/HfO_2 interface, Phys. Rev. B 87 (2013) 075325.
[6] M. Chang, M.S. Chen, A. David, S. Gandikota, S. Ganguli, B.E. Hayden, S. Hung, X. Lu, C. Mormiche, A. Noori, D.C.A. Smith, C.J.B. Vian, Novel metal gates for high κ applications, J. Appl. Phys. 113 (2013) 034107.
[7] B. Magyari-Köpe, S. Park, L. Colombo, Y. Nishi, K. Cho, Ab initio study of Al–Ni bilayers on SiO_2: implications to effective work function modulation in gate stacks, J. Appl. Phys. 105 (2009) 013711.
[8] Y.W. Chen, C.M. Lai, T.F. Chiang, L.W. Cheng, C.H. Yu, C.H. Chou, C.H. Hsu, W.Y. Chang, T.B. Wu, C.T. Lin, Effective work function modulation by aluminum ion implantation on Hf-based high-k/metal gate pMOSFET, IEEE Electron Device Lett. 31 (2010) 1290.
[9] C.K. Chiang, C.H. Wu, C.C. Liu, J.F. Lin, C.L. Yang, J.Y. Wu, S.J. Wang, Effects of La_2O_3 capping layers prepared by different ALD lanthanum precursors on flatband voltage tuning and EOT scaling in TiN/HfO_2/SiO_2/Si MOS structures, J. Electrochem. Soc. 158 (4) (2011) H447.
[10] W.J. Maeng, W.-H. Kim, J.H. Koo, S.J. Lim, C.-S. Lee, T. Lee, H. Kim, Flatband voltage control in p-metal gate metal-oxide-semiconductor field effect transistor by insertion of TiO_2 layer, Appl. Phys. Lett. 96 (2010) 082905.
[11] X. Luo, G. Bersuker, A.A. Demkov, Band alignment at the SiO_2/HfO_2 interface: group IIIA versus group IIIB metal dopants, Phys. Rev. B 84 (2011) 195309.
[12] L. Lin, J. Robertson, Atomic mechanism of electric dipole formed at high-κ:

SiO2 interface, J. Appl. Phys. 109 (2011) 094502.
[13] H. Zhu, G. Ramanath, R. Ramprasad, Interface engineering through atomic dopants in HfO_2-based gate stacks, J. Appl. Phys. 114 (2013) 114310.
[14] S. Guha, V. Narayanan, High-κ/metal gate science and technology, Annu. Rev. Mater. Res. 39 (2009) 181.
[15] K. Xiong, P. Delugas, J.C. Hooker, V. Fiorentini, J. Robertson, D.M. Liu, G. Pourtois, Te-induced modulation of the interface effective work function, Appl. Phys. Lett. 92 (2008) 113504.
[16] R. Gassilloud, C. Maunoury, C. Leroux, F. Piallat, B. Saidi, F. Martin, S. Maitrejean, A study of nitrogen behavior in the formation of Ta/TaN and Ti/TaN alloyed metal electrodes on SiO_2 and HfO_2 dielectrics, Appl. Phys. Lett. 104 (2014) 143501.
[17] J. Robertson, Interfaces and defects of high-κ oxides on silicon, Solid-State Electron. 49 (2005) 283.
[18] R.K. Pandey, R. Sathiyanarayanan, U. Kwon, V. Narayanan, K.V.R.M. Murali, Role of point defects and HfO_2/TiN interface stoichiometry on effective work function modulation in ultra-scaled complementary metal–oxide–semiconductor devices, J. Appl. Phys. 114 (2013) 034505.
[19] D. Lim, R. Haight, M. Copel, E. Cartier, Oxygen defects and Fermi level location in metal-hafnium oxide-silicon structures, Appl. Phys. Lett. 87 (2005) 072902.
[20] A.A. Knizhnik, I.M. Iskandarova, A.A. Bagatur'yants, B.V. Potapkin, L.R.C. Fonseca, Impact of oxygen on the work functions of Mo in vacuum and on ZrO_2, J. Appl. Phys. 97 (2005) 064911.
[21] Q. Li, Y.F. Dong, S.J. Wang, J.W. Chai, A.C.H. Huan, Y.P. Feng, C.K. Ong, Evolution of schottky barrier heights at Ni/HfO_2 interfaces, Appl. Phys. Lett. 88 (2006) 222102.
[22] J.K. Schaeffer, L.R.C. Fonseca, S.B. Samavedam, Y. Liang, P.J. Tobin, B.E. White, Contributions to the effective work function of platinum on hafnium dioxide, Appl. Phys. Lett. 85 (2004) 1826.
[23] D. Gu, S.K. Dey, P. Majhi, Effective work function of Pt, Pd, and Re on atomic layer deposited HfO_2, Appl. Phys. Lett. 89 (2006) 082907.
[24] C.-H. Lu, G.M.T. Wong, M.D. Deal, W. Tsai, P. Majhi, C.O. Chui, M.R. Visokay, J.J. Chambers, L. Colombo, B.M. Clemens, Y. Nishi, Characteristics and mechanism of tunable work function gate electrodes using a bilayer metal structure on SiO_2 and HfO_2, IEEE Electron Device Lett. 26 (7) (2005) 445.
[25] H. Yang, Y. Son, S. Baek, H. Hwang, H. Lim, H.-S. Jung, Ti gate compatible with atomic-layer-deposited HfO_2 for n-type metal-oxide-semiconductor devices, Appl. Phys. Lett. 86 (2005) 092107.
[26] H.Y. Yu, C. Ren, Y.-C. Yeo, J.F. Kang, X.P. Wang, H.H.H. Ma, M.-F. Li, D.S.H. Chan, D.-L. Kwong, Fermi pinning-induced thermal instability of metal-gate work functions, IEEE Electron Device Lett. 25 (5) (2004) 337–339.
[27] Y.F. Dong, S.J. Wang, J.W. Chai, Y.P. Feng, A.C.H. Huan, Impact of interface structure on Schottky-barrier height for Ni/ZrO_2(001) interfaces, Appl. Phys. Lett. 86 (2005) 132103.
[28] J. Robertson, O. Sharia, A.A. Demkov, Fermi level pinning by defects in HfO_2 -metal gate stacks, Appl. Phys. Lett. 91 (2007) 132912.
[29] Y. Akasaka, G. Nakamura, K. Shiraishi, N. Umezawa, K. Yamabe, O. Ogawa, M. Lee, T. Amiaka, T. Kasuya, H. Watanabe, T. Chikyow, F. Ootsuka, Y. Nara, K. Nakamura, Modified oxygen vacancy induced fermi level pinning model extendable to P-metal pinning, Jpn. J. Appl. Phys. 45 (2006) L1289.
[30] S.R. Bradley, K.P. McKenna, A.L. Shluger, The behaviour of oxygen at metal electrodes in HfO_2 based resistive switching devices, Microelectron. Eng. 109 (2013) 346.
[31] E. Cho, S. Han, Electronic structure of Pt/HfO_2 interface with oxygen vacancy, Microelectron. Eng. 88 (2011) 3407.
[32] A.A. Demkov, Thermodynamic stability and band alignment at a metal–high-κ dielectric interface, Phys. Rev. B 74 (2006) 085310.
[33] O. Sharia, K. Tse, J. Robertson, A.A. Demkov, Extended Frenkel pairs and band alignment at metal-oxide interfaces, Phys. Rev. B 79 (2009) 125305.
[34] A. O'Hara, G. Bersuker, A.A. Demkov, Assessing hafnium on hafnia as an oxygen getter, J. Appl. Phys. 115 (2014) 183703.
[35] K.J. Park, G.N. Parsons, Selective area atomic layer deposition of rhodium and effective work function characterization in capacitor structures, Appl. Phys. Lett. 89 (2006) 043111.
[36] E. Cho, B. Lee, C.-K. Lee, S. Han, S.H. Jeon, B.H. Park, Y.-S. Kim, Segregation of oxygen vacancy at metal-HfO_2 interfaces, Appl. Phys. Lett. 92 (2008) 233118.
[37] H.-K. Noh, Y.J. Oh, K.J. Chang, Effect of O-vacancy defects on the schottky barrier heights in Ni/SiO_2 and Ni/HfO_2 interfaces, Phys. B 407 (2012) 2907.
[38] X.F. Wang, L. He, S. Halas, T. Pienkos, J.G. Lin, T. Durakiewicz, The canonical work function-strain relationship of the platinum metal: a first-principles approach to metal-gate transistor optimization, Appl. Phys. Lett. 102 (2013) 223504.
[39] M. Peressi, N. Binggeli, A. Baldereschi, Band engineering at interfaces: theory and numerical experiments, J. Phys. D. Appl. Phys. 31 (1998) 1273.
[40] T.C. Leung, C.L. Kao, W.S. Su, Y.J. Feng, C.T. Chan, Relationship between surface dipole, work function and charge transfer: some exceptions to an established rule, Phys. Rev. B 68 (2003) 195408.
[41] K.Y. Tse, D. Liu, J. Robertson, Electronic and atomic structure of metal-HfO_2 interfaces, Phys. Rev. B 81 (2010) 035325.
[42] H. Zhu, R. Ramprasad, Effective work function of metals interfaced with dielectrics: a first-principles study of the Pt-HfO_2 interface, Phys. Rev. B 83 (2011) 081416(R).
[43] M. Bokdam, P.A. Khomyakov, G. Brocks, P.J. Kelly, Field effect doping of graphene in metal| dielectric| graphene heterostructures: a model based upon first-principles calculations, Phys. Rev. B 87 (2013) 075414.
[44] G. Kresse, J. Joubert, From ultrasoft pseudopotentials to the projector augmented-wave method, Phys. Rev. B 59 (1999) 1758.
[45] J.P. Perdew, K. Burke, M. Ernzerhof, Generalized gradient approximation made simple, Phys. Rev. Lett. 77 (1996) 3865.
[46] G.G. Xu, Q.Y. Wu, Z.G. Chen, Z.G. Huang, R.Q. Wu, Y.P. Feng, Disorder and surface effects on work function of Ni-Pt metal gates, Phys. Rev. B 78 (2008) 115420.
[47] K.H. Zhong, G.G. Xu, Y.M. Cheng, K.Q. Tang, Z.G. Chen, Z.G. Huang, A novel spin modulation of work function for C adsorbed Cr/Fe(001) metal gate, AIP Adv. 2 (2012) 042134.
[48] K.H. Zhong, G.G. Xu, J.-M. Zhang, Z.G. Huang, Effects of strain on effective work function for Ni/HfO_2 interfaces, J. Appl. Phys. 116 (2014) 063707.
[49] G.G. Xu, Q.Y. Wu, Z.G. Chen, Z.G. Huang, Y.P. Feng, Effects of surface alloying and orientation on work function of MoTa metal gate, J. Appl. Phys. 106 (2009) 043708.
[50] J.-M. Zhang, W. Ming, Z. Huang, G.-B. Liu, X. Kou, Y. Fan, K.L. Wang, Y. Yao, Stability, electronic, and magnetic properties of the magnetically doped topological insulators Bi_2Se_3, Bi_2Te_3, and Sb_2Te_3, Phys. Rev. B 88 (2013) 235131.
[51] J. Wang, H.P. Li, R. Stevens, Hafnia and hafnia-toughened ceramics, J. Mater. Sci. 27 (20) (1992) 5397.
[52] Y.F. Dong, Y.P. Feng, S.J. Wang, A.C.H. Huan, First-principles study of ZrO_2/Si interfaces: energetics and band offsets, Phys. Rev. B 72 (2005) 045327.
[53] W.L. Scopel, Antônio J.R. da Silva, W. Orellana, A. Fazzio, Comparative study of defect energetics in HfO_2 and SiO_2, Appl. Phys. Lett. 84 (2004) 1492.
[54] C.G. Van de Walle, R.M. Martin, Theoretical calculations of heterojunction discontinuities in the Si/Ge system, Phys. Rev. B 34 (1986) 5621.
[55] A. Baldereschi, S. Baroni, R. Resta, Band offsets in lattice-matched heterojunctions: a model and first-principles calculations for GaAs/AlAs, Phys. Rev. Lett. 61 (1988) 734.
[56] L. Colombo, R. Resta, S. Baroni, Valence-band offsets at strained Si/Ge interfaces, Phys. Rev. B 44 (1991) 5572.
[57] K.T. Chan, J.B. Neaton, M.L. Cohen, First-principles study of metal adatom adsorption on graphene, Phys. Rev. B 77 (2008) 235430.